Results from Cs activated GaN photocathode development for MCP detector systems at NASA GSFC

Timothy Norton[a*], Bruce Woodgate[b], Joseph Stock[c], George Hilton[a], Mel Ulmer[d]
[e]Shahid Aslam, [f]R.D Vispute

[a]Science Systems and Applications Inc , Lanham MD 20706 / Goddard Space Flight Center, Code 681, Greenbelt, MD 20771
[b]Goddard Space Flight Center, Code 681, Greenbelt, MD 20771
[c]Swales Aerospace Inc, Beltsville MD 20705
[d]Northwestern University, Evanston, IL 60208
[e]Raytheon ITSS/Goddard Space Flight Center, Greenbelt, MD 20771
[f]University of Maryland, Physics Department
College Park, MD 20742-4111

ABSTRACT

We describe the development of high quantum efficiency UV photocathodes for use in large area two dimensional microchannel plated based, detector arrays to enable new UV space astronomy missions. Future UV missions will require improvements in detector sensitivity, which has the most leverage for cost-effective improvements in overall telescope/instrument sensitivity. We use new materials such as p-doped GaN, AlGaN, ZnMgO, SiC and diamond. We have currently obtained QE values > 40 % at 185 nm with Cesiated GaN, and hope to demonstrate higher values in the future. By using controlled internal fields and nano-structuring of the surfaces, we plan to provide field emission assistance for photoelectrons while maintaining their energy distinction from dark noise electrons. We will transfer these methods from GaN to ZnMgO a new family of wide band-gap materials more compatible with microchannel plates. We also are exploring technical parameters such as doping profiles, internal and external field strengths, angle of incidence, field emission assistance, surface preparation, etc.

Keywords: detectors, photon-counting, photocathodes, negative electron affinity, microchannel plates,

1. INTRODUCTION

Micro-channel based photon-counting detectors remain the dominant technology for UV space based astronomy applications due to key performance parameters including large format (in area and pixel count), low background, zero read noise, long-wavelength rejection, radiation tolerance, and room temperature operation. Current and future missions which rely upon this technology include HST-STIS, GALEX, COS, EUVE, XMM-OM, CHIPS ,FAUST. With the recent development of silicon based MCPs, Beetz[1] advantages in geometrical uniformity, background rate, and reduced production costs, promise to revitalize this technology. However more importantly their ability to serve as host substrates for a new class of high quantum efficiency Negative Electron Affinity (NEA) photocathodes such as GaN, AlGaN, SiC and ZnMgO (due to their higher processing temperatures and cleanliness compared with glass MCPs) may allow much greater improvements over existing available detector quantum efficiency in the near and far UV regions.

[*]Correspondence: E-mail: tjn@pulsar gsfc.nasa.gov; Phone: 301-286-6541; FAX: 301-286-1752 .

1.1 GaN photoemissive layers

The primary characteristics for high QE GaN/AlGaN III-V material photocathodes for UV astronomy are :-

- Material must be deposited on sapphire or Silicon carbide for good lattice matching
- That it must be p-type to allow surface band-bending leading to high NEA and QE.
- high carrier concentration and mobility leading to high conductivity and QE
- tunable long-wavelength response via band-gap modifying AlN molar concentration to allow solar-blind cut-off around 320 nm.

To enable high electron escape probability from a semi-conductor based photoemissive layer and hence high quantum efficiency the energy difference between the bottom of the semiconductor conduction band and the vacuum level must be as low as possible to produce effective negative electron affinity, described further by Bell[2].
P-doping produces a Fermi level near the top of the bulk material valence band. As the positively charged surface is approached a depletion region is produced in which positively charged majority carrier holes are repelled leaving exposed fixed negative charges. This produces a downward band-bending effect resulting in a reduction in the electron affinity. Treatment of the surface with cesium and oxygen further reduces the vacuum level leading to effective NEA.

Magnesium is the preferred p-type dopant for GaN and AlGaN . However Mg has a high ionization energy of about 200 meV.which leads to <1% ionization at room temperature therefore over 100 x dopant concentration is needed to acquire a nominal hole density. This leads to required dopant concentration levels of $> 10^{20}$ cm $^{-3}$ close to the solubility limit of Mg in GaN. This produces poor hole mobility and very high resistivity in the material and subsequently very low photon-yield. Furthermore GaN is easier to dope more highly than AlGaN (which is desirable for UV astronomy due to the tunable aspect of its band-gap by increased molar AlN concentration leading to optimised long-wavelength cutoff) since the activation energy of Mg increases with additional Al molar concentration. Current realistic levels of Mg doping of GaN lie in the range $1 – 5 \times 10^{17}$ cm $^{-3}$

1.2 Surface activation with Cs and Oxygen

It has been long known that surface activation with Cs and oxygen are known to reduce the surface barrier potential of non-NEA photocathode materials leading to higher QE. For example the standard bi-alkali photocathode, (NaKSb) material when deposited and activated with a monolayer of Cs leads to a higher QE (particularly at wavelengths >500nm) photocathode, the ubiquitous S.20 (NaKSb:Cs). These layers show QE values up to 25 % at 400 - 500 nm. The more 'recently' developed Gen III night vision photocathode III-V material GaAs is also activated with Cs and Oxygen leading to QE > 40 % at 500 nm. Therefore it is believed that the higher band-gap III-V materials which have intrinsic NEA such as GaN and AlGaN for UV applications can be similarly enhanced. Literature such as Uebring and James[3] suggest that a heterojunction model applies in the case of Cs_2O grown on III-V semi-conductors such as GaAs and GaN. They go on to predict the maximum escape probability of different III-V semi-conductors coated with Cs_2O. They describe a process in which cesium oxide layers are grown on GaAs by first exposing the layer to Cs vapor until a maximum photo-yield is obtained. Then the layer is exposed alternately to oxygen and Cs , each time optimizing the photoyield. The Cs was evolved via a standard getter based , chromate salt source. The oxygen was admitted via a leak valve from a manifold filled with high purity oxygen. They report optimum levels of photo-yield were obtained with 250 second cycles of Cs exposure combined with 6×10^{-6} torr.sec leak rate of oxygen. This was for activation of a GaAs layer and may not be applicable for GaN layer activation however we have used these as useful starting points for experiments aimed at optimization of Cs treated GaN substrates at GSFC.

One of the major problems in GaN photocathode development is finding a suitable substrate match. There are two materials which have been found to produce minimum lattice defect mismatches with GaN, these are sapphire and silicon carbide. It is not clear how a sapphire layer may be deposited at the input of an Si-MCP however, conversion of the input silicon surface substrate of an Si-MCP to SiC for GaN photocathode growth may be achieved by high > 1000 degrees C temperature treatment with methane gas. Although this is clearly theoretically possible a number of questions remain including how uniform this layer may be and to what depth it may penetrate the MCP pores. Previous experience with diamond layer deposition on Si-MCP structures has lead to highly non-uniform layer deposition and poor pore penetration. These problems must be addressed and resolved in conjunction with Nanosciences Inc before high QE GaN photocathodes can be succesfully matched to new Si-MCP structures

2. SETUP AND FACILITIES

Figure 1. shows the UHV vacuum system used at GSFC to cesiate the candiate photocathode materials and related optical equipment for calibrating the photocathode following cesiation. Vacuum levels of less than 1 x 10^{-9} torr are achievable in this system following a 24 hr. 350C bakeout. Mounted near the center of the vacuum system is an assembly that holds the (SAES) evaporative cesium sources and holds the photocathode sample directly above the Cs source. The photocathode (on its substrate) is mounted in a stainless fixture and is electrically isolated from the surrounding hardware, and is DC biased for photoelectron collection. Photocurrent measurements are made with a Keithley picoammeter and are digitally stored with LabView as are other system parameters such as pressure, temperature, and RGA spectra.

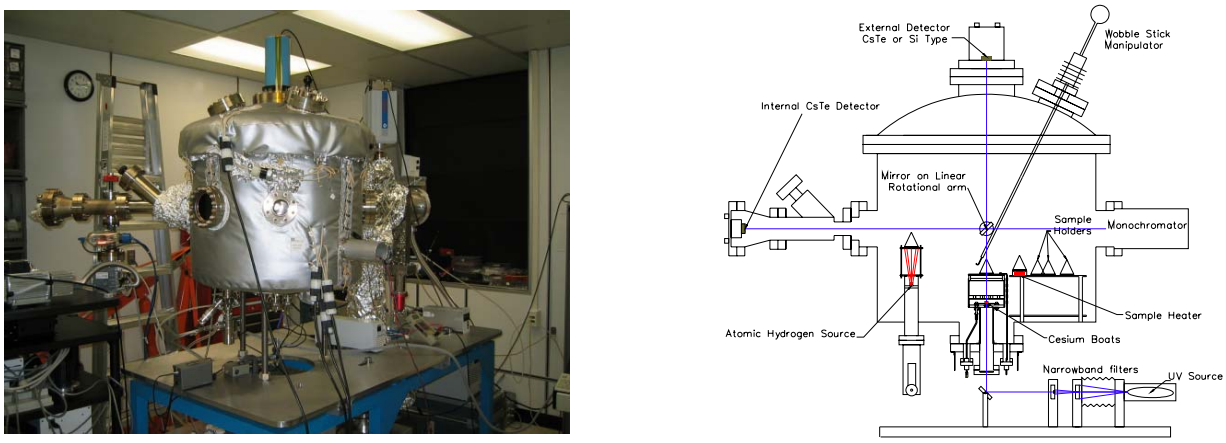

Fig. 1: GSFC UHV photocathode processing chamber

Illumination of the sample during cesiation and calibration is from a pencil-type Hg line source mounted outside the vacuum chamber. Narrowband filters provide isolation of specific calibration lines. We also have the capability to mount a vacuum monochromator to the system to allow a more thorough wavelength survey of the quantum efficiency (including FUV); implementing this system is currently underway. Reference detectors for calibration are mounted both internally and externally to the chamber, usage depends on the wavelength of interest and illumination method. The internal detector is CsTe and is used for calibrating below 300nm and is accessible by diverting the pencil beam of UV from the lamp using an internal mirror mounted on a rotation manipulator. This detector is valved off during cesiation. Typically a CsTe or Silicon PIN detector is also mounted external to the chamber in a direct line-of-sight to the sample UV flux. This is particularly useful for UV reference detector measurements during cesiation and is the configuration used for long wavelength calibration using the silicon photodiode.

An atomic hydrogen source and a high temperature heater are located in the vacuum system to provide *in situ* final cleaning of the surface of the sample prior to Cs activation. The atomic hydrogen source creates atomic hydrogen by thermally cracking H_2 bled into the source by a leak valve and is capable of producing H fluxes at the sample of ~10^{16} $cm^{-2}s^{-1}$. The flux of atomic hydrogen converts carbon and oxygen based contaminants on substrate surfaces (known to be particularly deleterious to photoemission) into volatile species which evaporate readily at relatively low temperatures. A resistive disk heater allows high temperature (>800 °C) heating of the sample to remove adsorbed hydrogen
carbon and oxygen and other species remaining on the surface. Samples are moved manually between these locations and the cesiation assembly using a bellows manipulator. Multiple samples can be loaded into the system at one time and individually selected for processing and calibration.
Facilities for cleaning and handling include a class 1000 clean room with a flow bench for handling samples and other hardware loaded into the UHV system. Sample preparation is done in a semiconductor processing facility at GSFC. In this facility the GaN (or other material) wafers are cut to size, plated with electroding (if desired), and acid (pirahna and HF) cleaned. GSFC also has facilities for material characterization and microscopy including Atomic Force Microscopy (AFM).

3. PROCEDURE

Prior to installation into the UHV vacuum system photocathode samples are piranha acid (H_2SO_4 : H_2O_2) cleaned followed by an HF acid dip. The vacuum system is then baked at 350 C for 24 hrs and the cesium metal dispensers are outgassed below the firing current prior to any processing of the photocathodes. Just prior to cesiation of the photocathode, the surface is cleaned by exposure to atomic hydrogen for an extended period (3+ hrs.) and/or heating (> 500C). We are still in the process of evaluating the optimum parameters for this final cleaning, but generally we see an improvement in efficiency for samples that are subjected to this final cleaning vs. samples that are not.
The clean photocathode surface is then activated by exposure to cesium while the photocurrent is monitored. Once the photocurrent is peaked the exposure is stopped. Following this initial cesium exposure the chamber is backfilled with O_2 to a partial pressure of ~5 x 10^{-8} Torr until the signal falls to a desired point. Alternating O_2/cesium exposures, (figure 2.) are then continued until a peak signal is reached. We generally find that for GaN, >90% of the peak signal is attained after 2 cycles. High-rejection narrowband filters are installed to isolate specific Hg lines in order to calibrate the quantum efficiency of the photocathode vs. wavelength. Elements outside of the vacuum system must be purged with dry N_2 for any measurements below 200nm and care is taken to ensure that the UV beam is fully on both the sample and reference detector.

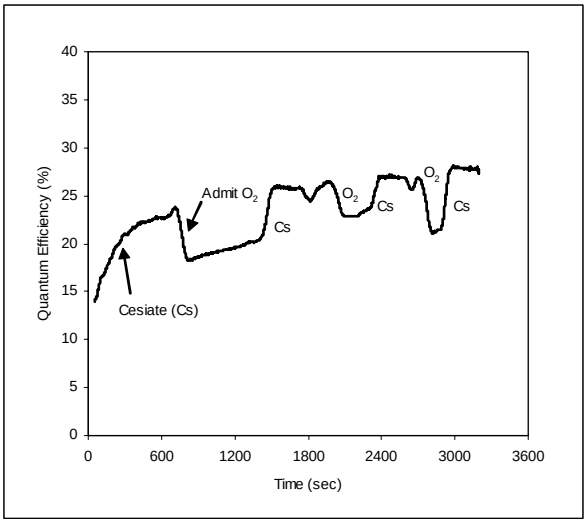

Fig. 2: Cesiation and Oxygenation of GaN photocathodes

4. RESULTS

Table 1. shows the results of Cs activation of a number of GaN layers manufactured by Northwestern Univ (NWU) and SVT Associates (SVT) of varying thickness, cleaning regimes and Cs/O yo-yo activation cycles. It is not obvious from the currently limited parameter data available of the effect of different Mg dopant levels , thickness , minority carrier mobility and resistivity. However the effect of the adoption of piranha and HF wet etch surface preparation is clear. Much higher QE values are obtained for substrates pre-wet etched with these materials leading to a conclusion that these techniques are essential in order to remove C and O surface contaminants. The cesiation and oxygenation activation cycles seem to be very predictable in order to produce high QE GaN photocathode layers. The beneficial effect of atomic Hydrogen and thermal desorption of contaminants is not yet fully determined. The role of MOVCD (NWU) vs MBE (SVT) growth of layers seems not to be a major factor in ultimate layer QE. Figure 3. shows the quantum efficiency vs wavelength for both cesiated SVT and NWU GaN wafer material measured in opaque mode. For comparison the QE curve for the CsTe semi-transparent photocathode employed on HST-STIS, NUV MAMA detector is shown.

Properties					Surf. prep.			Activation	Result
Mfg.	Thk.	Res. Ω-cm	Hole Conc. $x10^{17}$ cm^{-3}	Mob. cm^2/Vs	Pirahna & HF	H	Heat >500C	Activation	QE % @ 254 nm
SVT	0.1 μm	-	>5	-	-	-	-	Cs/O/Cs/O/Cs	1.3
SVT	0.1 μm	-	>5	-	-	-	-	Cs	1.3
SVT	0.1 μm	-	>5	-	-	-	x	Cs	1.2
SVT	0.1 μm	-	>5	-	-	x	-	Cs/O/Cs	2.2
SVT	0.1 μm	-	>5	-	-	x	x	Cs/O/Cs/O/Cs	14.5
SVT	0.1 μm	-	>5	-	-	x	x	Cs/H/Cs/H/Cs	11.5
SVT	0.1 μm	-	>5	-	-	-	x	Cs	1.0
SVT	0.1 μm	-	>5	-	-	x	x	Cs/O/Cs/O/Cs/O/Cs	15.0
SVT	0.3 μm	-	>5	-	-	-	-	Cs	1.2
SVT	0.3 μm	-	>5	-	-	-	-	-	-
NWU	0.1 μm	16.3	2	1.88	x	x	x	Cs/O/Cs/O/Cs/O/Cs	28.0
NWU	1 μm	7.06	1	8.75	x	-	-	Cs	3.8
SVT	0.3 μm	-	>5	-	-	-	-	-	-
SVT	0.1 μm	-	>5	-	x	-	-	Cs/O/Cs/O/Cs	22.0
SVT	0.1 μm	-	>5	-	x	-	x	Cs/O/Cs/O/Cs	19.0
SVT	0.3 μm	-	>5	-	x	x	x	Cs/O/Cs/O/Cs	24.0
SVT	0.3 μm	-	>5	-	x	-	x	Cs/O/Cs/O/Cs	24.0
NWU	0.1 μm	16.3	2	1.88	x	x	x	Cs/O 10x	32.0
NWU	0.1 μm	9.14	4	1.68	x	-	-	Cs/O/Cs/O/Cs/O/Cs	30.0
SVT	0.3 μm	-	>5	-	x	x	x	Cs/O/Cs/O/Cs	24.0
SVT	0.1 μm	-	>5	-	x	x	x	Cs/O/Cs/O/Cs	24.0
SVT	0.2 μm	-	>5	-	x	x	x	Cs/O/Cs/O/Cs/Cs/O/Cs	30.0
SVT	0.3 μm	-	>5	-	x	x	x	Cs/O/Cs/O/Cs	18.0

Table. 1: Cesiated GaN photocathodes – Sample parameters and quantum efficiency results

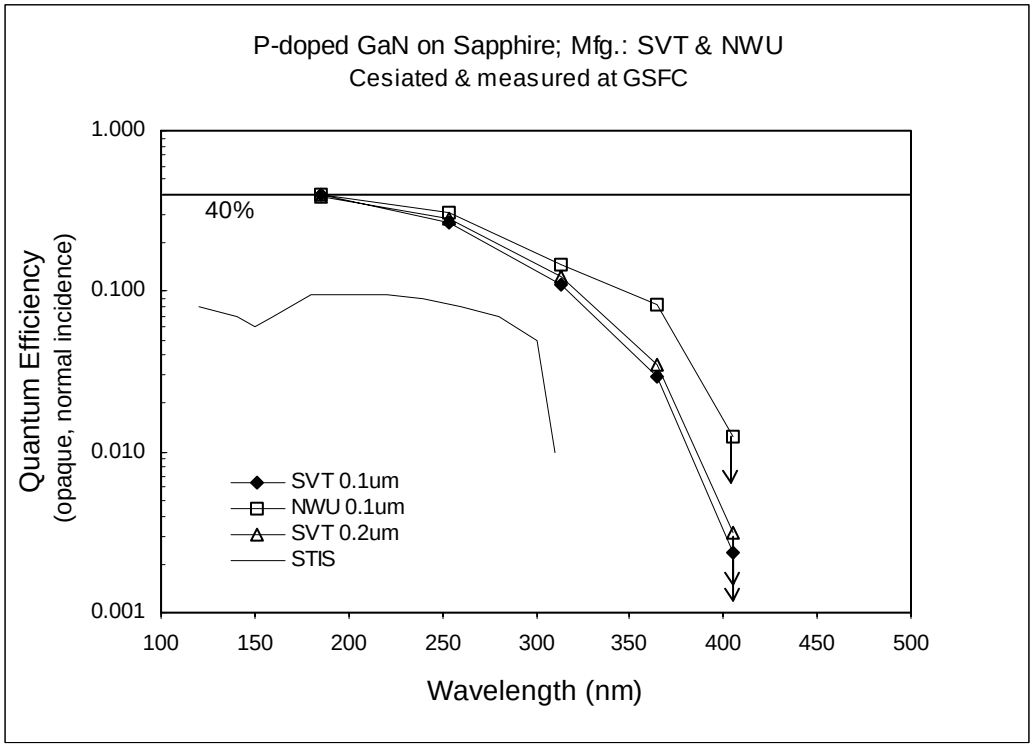

Fig. 3: Quantum efficiency vs wavelength of Cesiated GaN photocathodes.

4.1 Surface Morphology

We have carried out Atomic Force Microscopy (AFM) analysis of the GaN substrate surface in order to determine the surface morphology of the layers before and after processing. AFM is a non-destructive technique able to distinguish features in a surface of size < 20 nm. We carried out analysis of GaN substrates before and after cleaning and Cs activation. It is clear that for layers < 100nm there are many deep 'voids in the material, Figure 4. Electron Dispersive Spectroscopy (EDS) analysis, figure 5. shows that features are present with almost complete depletion of GaN down to the sapphire base substrate.

Fig. 4: AFM analyzed surface morphology of GaN substrates.

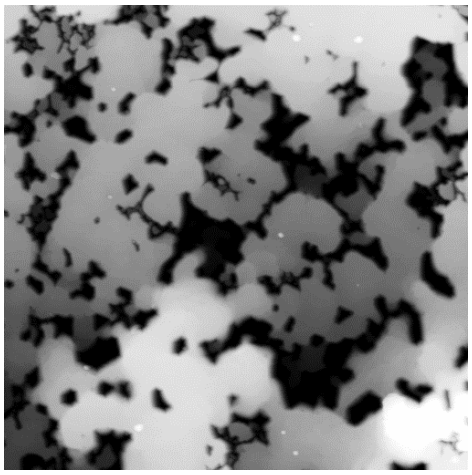

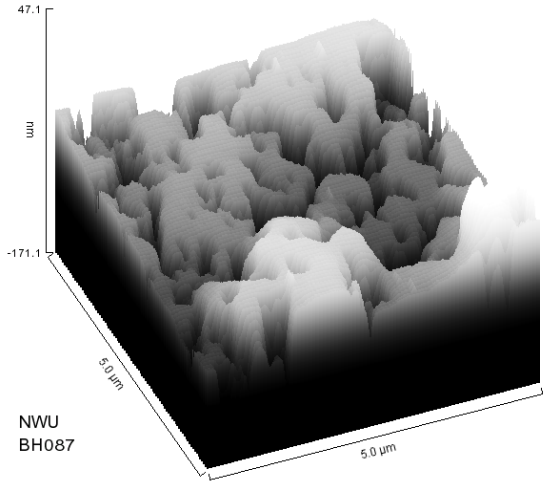

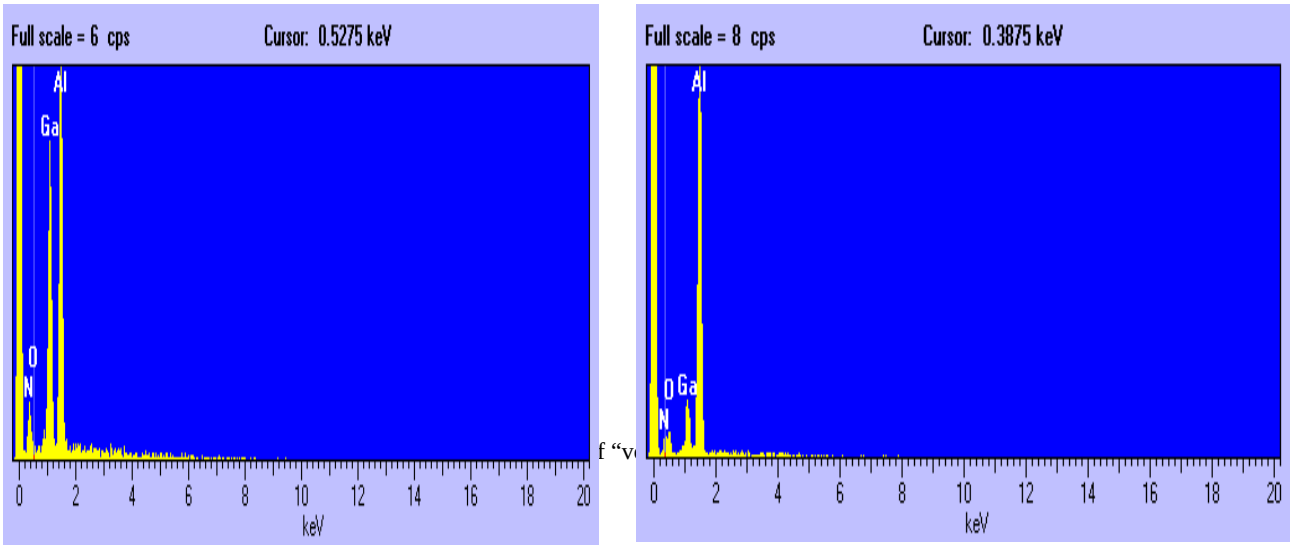

Fig. 5: EDS analysis of GaN substrates outside and inside of "voids". – showing GaN depletion

In order to determine whether the voids in the GaN were caused or exacerbated by our wet-etch cleaning of the material we carried out AFM measurements of the wafers before and after etching and for extended etching periods. Image histogram analysis revealed that the etching has very little effect on the structure. We therefore believe this morphology is due to incomplete material growth particularly for such thin layers < 0.3 μm.

5. STATUS AND PLANS

5.1 Field enhanced photoemission

It has been well known for some time that application of a field to a III-V photocathode such as GaAs can considerably enhance the QE of the layer, Bell[4] It has been shown that by applying an high external field photocathode quantum efficiency improvement of up to two-fold can be obtained.

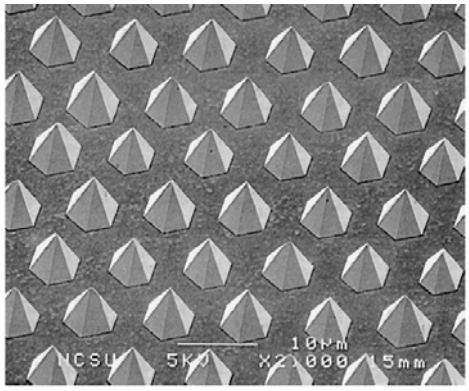

Figure 6 . Pyramidal structures in GaN

Careful use of structured field enhancing surfaces such as those developed for electron beam lithography applications may enhance QE while limiting any increase in dark noise. Nemanich[5] have made sharp pyramid structures in GaN (Fig 6), and demonstrated preferential photo-electron emission from the points and edges. They show that a distinction can be made between the photoelectrons and internally generated electrons. This work was done in n-doped GaN, without cesiation, so we expect that combining p-doped GaN and cesiation with surface structure may be more effective. We plan to construct much finer scale structures (~ 0.2 microns) than made by Nemanich, in order to make many emitting structures per pixel for photometric uniformity, and to decrease photoelectron transport distances between the production and emission sites. Such structures may be produced in a number of ways. Fine features may be produced by etching of the sapphire substrate and then depositing GaN layers. Alternatively etching of GaN around etch stops in the material may produce the desirable morphology for enhancing photoelectron emission.

5.2 Co-doped GaN material

A potential solution to the problem of limited p-type doping of GaN with Mg described earlier has been identified by a number of workers. That is co-doping the material with elements such as hydrogen, zinc, beryllium, selenium, silicon and oxygen. It is argued that co-doping with these materials produces complexes that lead to enhanced hole mobility due to the formation of impurity complexes that act as short range dipole scatterers rather than long range Coulomb scattering which is dominant in Mg only doped films. Kim et al[6] have demonstrated GaN films , co-doped with Zn showing a low resistivity ((0.7cm) and high hole concentration (8.5 x 10^{17} cm^{-3}). Ulmer[7] et al have followed this work with proposals to co-dope GaN materials intended for photocathode use with oxygen to enhance the conductivity and ultimately quantum yield of the layer. We have recently received co-doped Mg-O material from Northwestern University and hope to process this in the near future. We will compare the results we get with our existing singly doped wafers to determine if higher dopant concentrations producing improved surface band-bending and hence greater QE may be realized.

5.3 Alternative photocathode materials

ZnMgO: The University of Maryland have been developing a new material system, ZnMgO, that has a wider range of tunable band gaps (table 2) than GaN and AlGaN, and is potentially much easier to deposit on various substrates. Subsequently we intend to investigate the applicability of ZnMgO as a UV photocathode.

Comparison of crystal systems:	InN-GaN-AlN	CdO-ZnO-MgO
Band gap range	1.8 – 6.2 eV	2.8 – 8.0 eV
Cutoff wavelength	690 – 200 nm	440 – 154 nm
Single material band gap	GaN: 3.4 eV	ZnO: 3.3 eV
Exciton energy	28 meV	60 meV

Table. 2: GaN vs ZnMgO material parameters

This system has direct and tunable bandgaps from 2.8-7.9 eV obtained by substitution of Cd or Mg into the Zn site – the gap can be lowered with Cd or increased with Mg . Although this material technology is new, extensive work has been done at UMd, who have demonstrated, using pulsed laser deposition (PLD), some of the finest quality ZnMgO films on a variety of substrates and buffer layers Choopun et al.[8] The pulsed laser (25ns pulses from KrF at 248nm) is utilized for the ablation of composite target material to produce an intense plasma plume which then deposits onto the substrate, initially sapphire. The films have been grown epitaxially on sapphire, Si, and highly oriented on plastic, glass and GaAs. The optical band edge for the films has been shown to be very sharp . Layers of 0.3 microns thick are sufficient to absorb all UV photons at wavelengths below the band gap. The pulsed laser ablation method minimizes

contamination from containers compared to bulk heating methods because it removes surface material without significantly heating the bulk material or the container. The most outstanding feature of the laser deposited films is the high optical quality. The optical emission and the threshold for observation of super radiance (pre-lasing) from the ZnO films have been extremely impressive compared to figures for state of the art GaN obtained commercially from CREE Research. PLD can also offer relatively low temperature growth for ZnO; hence it is possible to develop lower temperature growth processes of ZnO on Si and GaAs. These studies clearly demonstrate the possibility of the integration of ZnO with III-V nitrides, Silicon, GaAs and other potential substrate materials to be used in this project. In addition, our Co-I's initial work demonstrates 1) lasing of ZnO film at room temperature, 2) low carrier concentration ($10^{17}/cm^3$) for undoped, high conductivity for doped, and high mobility in ZnO films and hence the possibility of p and n type doping (Choopun et al. 1999), and 3) ZnO band gap engineering by alloying with MgO (Choopun[8]).

We believe that ZnO compounds are more adaptable than the GaN because they can be grown at ~200C rather than ~1000C that is used for GaAlN growth. As well as on a wider selection of crystals, they can be grown on metals such as the metalization layers on microchannel plates) and even some polymers. ZnO can be doped with Al to densities between 10^{16} and 10^{21} cm^{-3}, whereas the GaN materials have only been doped to ~ 2 x 10^{18}. Electron mobilities are similar in the two groups of materials, with film mobilities 20 – 100 V cm^{-1} s^{-1}, and bulk mobilities 300 – 500 V cm^{-1} s^{-1}. P-type doping in ZnO and its compounds is under present investigation. The University of Maryland will supply ZnMgO and AlGaN samples produced by the laser ablation method for GSFC to apply the cesium and oxygen-cesium negative electron affinity surfaces. We will compare these with each other and the GaN/AlGaN substrates produced by other methods. We will also apply this method to deposit films onto silicon based microchannel plates, for direct use with an MCP image intensifier**.** At the time of writing recent activation of a laser pulse deposition (LPD) based un-p-doped ZnO substrate yielded a QE up to 0.4% at 254 nm. Although this is considerably low compared to GaN this result seems to offer significant hope that these layers may ultimately produce high QE when adequately p-doped.

6. DISCUSSION

Our investigations have demonstrated quantum efficiencies of > 30 % at 254nm and > 40 % at 185nm for cesiated GaN photocathode layers. Primarily we have determined that surface preparation via wet etch using piranha and HF cleaning is essential to remove residual C and O contaminants deleterious to efficient photoemission. We have also adopted atomic Hydrogen cleaning of these layers in addition to thermal desorption techniques up to 800 C in order to enable high QE values. Atomic force microscopy of these substrates has revealed clear incomplete layer growth for substrate depths < 100nm. It is not obvious as yet whether the QE values we have obtained are limited by decreased open area ratio values evident from this data, or indeed enhanced by increased field emission from these structures.
In order to acheive even higher QE values for these layers we believe that techniques including heterostructure design and substrate patterning enabling field enhanced QE emission may be required in order to attain photocathode QE values > 60 %. We intend to extend these techniques to II-VI materials such as ZnMgO in order to enable very high QE based photon counting detectors for new UV astronomy based missions.

ACKNOWLEDGMENTS

We acknowledge funding from NASA GSFC IR and D program

REFERENCES

1. Beetz, C.P., Boerstler, R., Steinbeck, J., Lemieux, B. and Winn, D.R., 2000, “Silicon-micromachined microchannel plates” Nuc. Instr. Methods, Phys. Res. A 442, 443

2. Bell, R.L, “Negative Electron Affinity Devices”, Clarendon Press, Oxford, 1973.

3. Uebbing, J.J., and James, L.W., 1970, “Behavior of Cesium Oxide as a low work function coating”, J. of Appl. Phys. 41, Number 11, 4505

4. Bell, R.L., James, L.W and Moon, R.L Appl. Phys. Lett **25**, 645 (1974)

5. R. J. Nemanich, P. K. Baumann, M. C. Benjamin, O. -H. Nam, A. T. Sowers, B. L. Ward, H. Ade and R. F. Davis Applied Surface Science, 130, June 1998, p.694

6. Ki Soo Kim, Chang Seok Oh, Myung Soo Han, Chi Sun Kim, Gye Mo Yang, Jeon Wook Yang, Chang-Hee Hong, Chang Joo Youn, Kee Young Lim, Hyung Jae Lee *MRS Internet J. Nitride Semicond. Res.* ***5S1***, W3.84 (2000).

7. Ulmer, M.P., Wessels, B.W., Shahedipour, F., Korotokov, R.Y., Joseph, C.L., and Nihashi, T., 2001, "Progress in the fabrication of GaN photocathodes", Proc. SPIE 4288, 246

8. Choopun, S., Vispute, R.D., Yang, W., Sharma, R.P., and Venkatesan, T., 2002, "Realization of cubic ZnMgO alloys above 5 eV by pulsed laser deposition", Appl. Phys. Lett. 80,1529